Tracing the groundwater inputs and water-mass mixing in the Coorong lagoons (South Australia) using strontium isotopes

Thesis submitted in accordance with the requirements of the University of Adelaide for an Honours Degree in Geology/Geophysics

Isaac Kell-Duivestein

November 2015

THE UNIVERSITY of ADELAIDE

TRACING THE GROUNDWATER INPUTS AND WATER-MASS MIXING IN THE COORONG LAGOONS (SOUTH AUSTRALIA) USING STRONTIUM ISOTOPES

TRACING GROUNDWATER INPUTS INTO THE COORONG WITH SR ISOTOPES

ABSTRACT

Analysis of elemental concentrations of strontium [Sr] and isotope ($^{87}Sr/^{86}Sr$ ratios) compositions measured in lagoonal waters sampled across the northern and southern parts of the Coorong Lagoon, South Australia are presented. These data are complemented by the analysis of major water inputs into the lagoon, including (i) Southern Ocean seawater, (ii) Murray River water, and (iii) a local groundwater source. Results of this study confirm that these different source endmembers have very distinctive $^{87}Sr/^{86}Sr$ signatures, which in turn allow quantification of their relative contributions to the water balance of the Coorong. Importantly, data confirms that at certain parts of the Coorong Lagoon (e.g., near Noonameena through Parnka Point) the magnitude of submarine groundwater discharge can be significant in localized areas, and by using $^{87}Sr/^{86}Sr$ a tracer along with bimodal isotope mixing equations, local contributions of these endmembers were able to be quantified. Specifically, results indicate that at these sites up to 38% of strontium in the North lagoon waters and up to 64% of strontium in the South lagoon waters originates from groundwater discharge, with the remaining part primarily derived from seawater. With the use of a further mass balance equation which also takes into account the Sr concentrations of the seawater and groundwater it was determined that the isotope signatures within the North Lagoon reflect groundwater inputs by volume of up to 80% in localized areas. In this contribution, we will discuss these new isotope and geochemical data within the context of the bimodal mixing processes, along with an observed initial decrease in the salinity of lagoonal waters observed in the northern parts of the Coorong before rapidly increasing to hypersaline waters further south through Parnka Channel and within the South Lagoon.

KEYWORDS

Coorong
Salinity
Submarine Groundwater Discharge (SGD)
Strontium Isotopes
Hyperbolic Mixing
Bimodal Mixing

TABLE OF CONTENTS

LIST OF FIGURES AND TABLES

1. INTRODUCTION

There have been many studies on the hydrology affecting the flow of water, and concomitantly the salt load, into and out of the Coorong lagoons. Collectively these studies have, to a degree, been able to characterize, model and quantify the hydrology and salinity of the lagoons. These have helped to explain past episodes of saline conditions and continue to offer hope that models and data may eventually have sufficient predictive power to quantify the various inputs of water into the Coorong and thus assist in making the best use of limited water allocations. However, although many studies such as those by (Brookes *et al.* 2009, Paton *et al.* 2009) have acknowledged that groundwater flows into the Coorong will have an effect on microhabitats within the Coorong, and possibly have some influence on the overall water salt balance, they have been unable to quantify the contribution made by groundwater to the overall water balance in the lagoons.

This pilot study aims to furnish an avenue of investigation that can assist in quantifying groundwater input into the lagoons by determining the isotopic ratios of radiogenic $^{87}Sr/^{86}Sr$ in the Coorong Lagoons and of potentially significant endmember contributors to their total water budget including; (i) local fresh groundwater discharge (ii) coastal Southern Ocean seawater and (iii) barrage release water from the Murray River and the Lower Lakes Alexandrina and Albert.

.

2. BACKGROUND

2.1 Coorong Profile

Spanning more than 120 km NW to SE along the South Australian coastline and marking the termination of the River Murray, Australia's largest river, is the Coorong. The Coorong is a major estuarine environment located within the southwest corner of the Murray Darling geological basin which is separated from the Southern Ocean by a narrow sand dune peninsula known as the Young Husband Peninsula and is connected to the sea only via a narrow channel at the very North of the system which is subject to infilling and scouring on a seasonal basis, dependent on whether water is flowing through the barrages or not (Haese *et al.* 2008, Brookes *et al.* 2009).

The Coorong has been classed as an inverse estuary (Pritchard 1952, Wolanski 1986, Webster 2010) because, unlike most lagoons that discharge to the sea along the length of their reach, its discharge to the sea occurs relatively close to the input source (Figure 1, Figure 2). As such, the near 100 km relatively narrow tail of the lagoon, running parallel to the coast and terminating in shallow mud flats, only gains a limited amount of water. As the entrance of the Northern Lagoon is adjacent to the barrages that separate it from Lake Alexandrina it has the benefit of receiving periodic discharges of fresh water. When barrage flows are limited the Northern Lagoon can still have the benefit of tidal inflows of Southern Ocean seawater to its head and some way down its reach southwards. Even though saline, this water can significantly lower the salinity of the water in the Northern Lagoon which at times is hypersaline towards its southern end. The Southern Lagoon is at best effectively only connected to the Northern Lagoon by a relatively narrow 100m wide winding channel that is over 1km long at Parnka

Point. Water entering the Southern Lagoon from the Northern Lagoon can have lower than seawater salinity when barrage flows are high, however not infrequently it is already hypersaline with respect to seawater. This inverse arrangement has led it to be further classified as a choked coastal lagoon (Knoppers 1994, Kjerfve *et al.* 1996, Webster 2010).

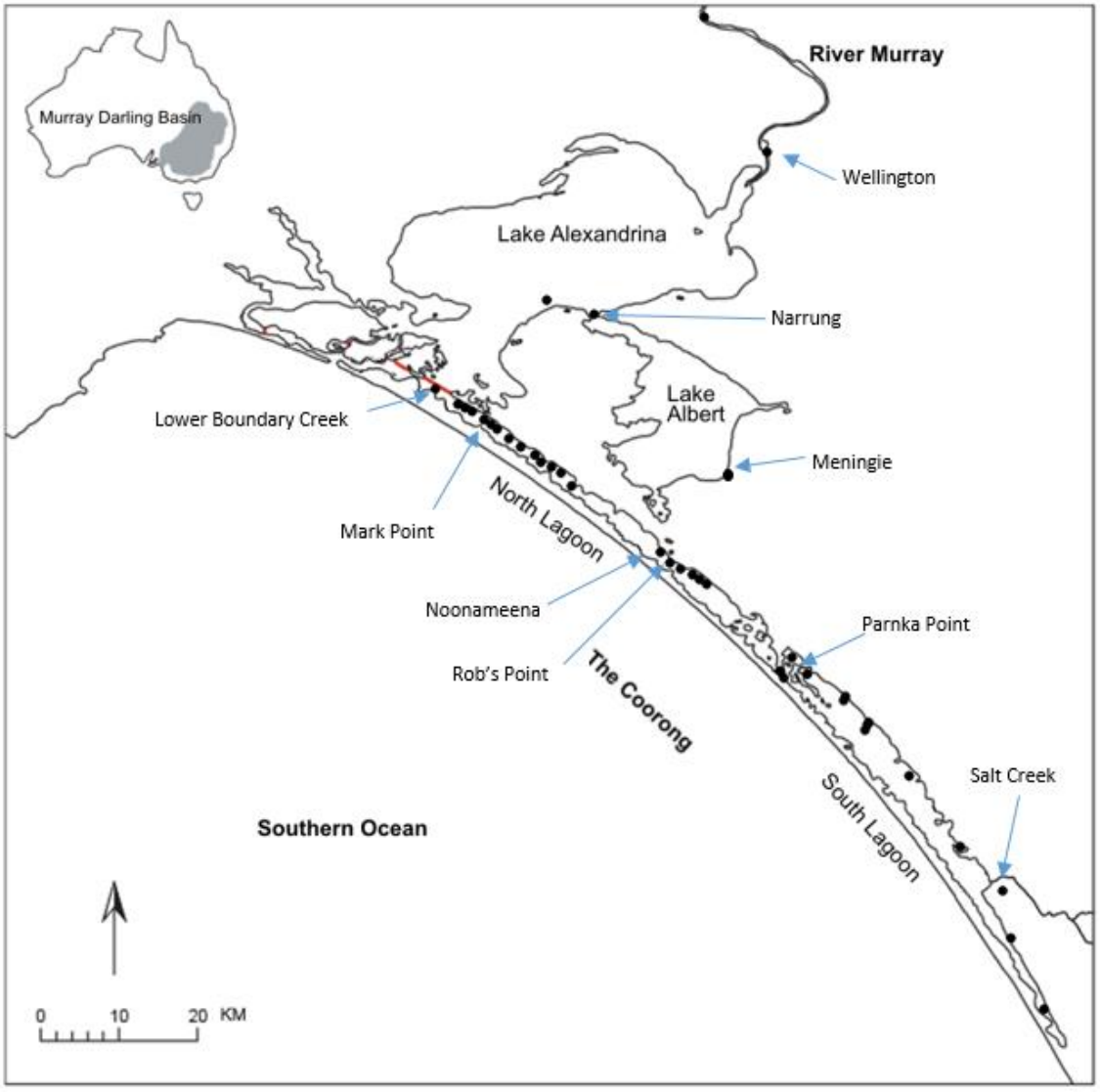

Figure 1: A map of the Coorong and Lower Lakes at the terminal end of the Murray River, South Australia. Sampling locations of study highlighted as well as key levers of Coorong hydrodynamics. Red bars in North between Pelican Point and Goolwa show barrage locations. Black points represent sampling sites. Modified from (Gillanders & Munro 2009).

Table 1: Summary of sampling locations and dates.

Sample ID	Specific	Latitude (S)	Longitude (E)	Sampling Date
SW	Open Ocean seawater from coastline	36.29073	139.70381	April 10, 2015
SL1A	Parnka Point	35.90195	139.39609	April 10, 2015
SL1B	Parnka Point	35.90114	139.39586	April 10, 2015
SL2	Parnka Point	35.88962	139.40544	April 10, 2015
SL3	Restricted Lake	35.89579	139.44009	April 10, 2015
SL4A	Lagoon widest part	35.91465	139.46185	April 10, 2015
SL4B	Lagoon widest part	35.91588	139.46091	April 10, 2015
SL5A	Possible seepage site (Ephemeral?)	35.95208	139.50243	April 10, 2015
SL5B	Seawater close to seepage	35.95341	139.50194	April 10, 2015
SL5C	Seawater further from seepage site	35.95502	139.50090	April 10, 2015
SL6	Woods Well	36.00515	139.55260	April 10, 2015
SL7	Policeman Point	36.05858	139.58607	April 10, 2015
SL8	Pelet/Milne Lake (Ephemeral Lake)	36.13676	139,13676	April 10, 2015
SL9	Site neat Halite Lake	36.15915	139.64642	April 10, 2015
SL10	Southern End of Coorong Lagoon	36.26485	139.71443	April 10, 2015
NL1	Robs Point	35.79718	139.64548	April 10, 2015
NL2	Robs Point	35.79716	139.31845	May 15, 2015
NL3	North of Robs Point ~1.5km	35.79007	139.30985	May 15, 2015
NL4	Near EMOHRUO	35.78446	139.30019	May 15, 2015
NL5	North of NL4 ~1.5km	35.78182	139.28700	May 15, 2015
NL6	Coorong Park	35.77216	139.27402	May 15, 2015
NL7	Near Noonameena	35.75518	139.26344	May 15, 2015
NLB1	North Northern Lagoon	35.69822	139.15980	May 15, 2015
NLB2	North Northern Lagoon	35.67260	139.15320	May 15, 2015
NLB3	North Northern Lagoon	35.68262	139.14620	May 15, 2015
NLB4	North Northern Lagoon	35.67605	139.13740	May 15, 2015
NLB5	North Northern Lagoon	35.66995	139.12760	May 15, 2015
NLB6	North Northern Lagoon	35.66373	139.11990	May 15, 2015
NLB7	North Northern Lagoon	35.65790	139.11060	May 15, 2015
NLB8	North Northern Lagoon	35.65177	139.10210	May 15, 2015
NLB9	North Northern Lagoon	35.64500	139.09100	May 15, 2015
NLB10	North Northern Lagoon	35.63857	139.08240	May 15, 2015
NLB11	North Northern Lagoon	35.63268	139.07230	May 15, 2015
NLB12	North Northern Lagoon	35.57472	139.06450	May 15, 2015
NLB13	North Northern Lagoon	35.61828	139.05170	May 15, 2015
NLB14	North Northern Lagoon	35.61092	139.03780	May 15, 2015
NLB15	North Northern Lagoon	35.59423	139.01530	May 15, 2015
LL1	Lake Albert from Pier in Meningie	-	-	May 15, 2015
LL2	Lake Alexandrina	35.50648	139.12962	May 15, 2015
LL3	Lower Lake connection at Narrung	35.51371	139.18536	May 15, 2015
MR1	Wellington ferry crossing	35.32936	139.38678	May 15, 2015
MR2	Below Murray Bridge main crossing	35.14715	139.31023	May 15, 2015
JWP2	Ground Water near Noonameena	35.78689	139.30640	June 25, 2015
BWP2	Ground Water near Noonameena	35.78459	139.30160	June 25, 2015

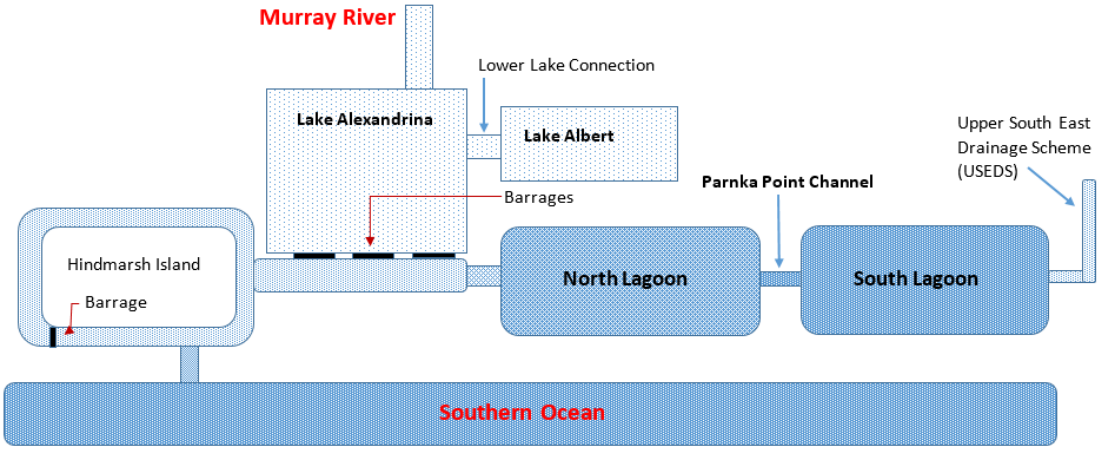

Figure 2: Schematic diagram showing Coorong lagoons and associated water bodies does not however include SGD or of precipitation as associated waterbodies. (Not to scale).

2.2 Degradation of an ecosystem

Increasing anthropogenic consumption of water from the Lower Lakes and Murray River since European settlement has led to reduction in freshwater fluxes to the Coorong lagoons. Coupled with severe drought from 2000-2010, the previous several decades have seen significant alteration to the hydrology of the system which has led to a sharp increase in salinity associated with lower water levels and progressive isolation from ocean flushes (Tulipani *et al.* 2014). This progressive shift in hydrology of the ecosystem has caused severe degradation of the ecological diversity of the Coorong (Shuttleworth *et al.* 2005, Commission 2006, Brookes *et al.* 2009). Because of the declining ecological condition of the region, it has become pressing on the stewards of this unique habitat to further investigate, characterize, quantify and model the complex dynamics and numerous variables inherent in managing the water quality and water regimes of the Coorong; and, hopefully, thereby improve its management.

2.3 Prior studies on submarine groundwater discharge (SGD)

There have been many studies that have characterised and quantified the salinity gradients of the Coorong lagoons; in general, reporting a transient range of salinities from fresh water and seawater inputs near the mouth and top end of the Northern Lagoon, and a gradual, if somewhat punctuated, increasing salinity, or hyper salinity, to the south end of the Southern Lagoon (Commission 2006, Brookes *et al.* 2009, Paton *et al.* 2009). However, as useful as many of the salinity measurements have been, they have been limited by their inability to resolve spatial and temporal differences of salinity with high resolution. Similarly, studies aiming to establish a clearer understanding of the hydrodynamics of the Coorong such as a recent study by (Webster 2010) have also been limited by the complexity of the system and the availability of extensive spatial and temporal data detailing inflows and outflows of water and the mixing of waters within the lagoons. The former limitations have possibly been a reason as to why sub marine groundwater discharges (SGD) may have been but poorly considered in a number of studies. Many have either discounted the contribution of SGD as relatively insignificant, or, having noted it as significant but have not quantified its contribution to the geochemistry of the Coorong lagoonal waters. Webster (2010), for instance, dismissed the contribution of SGD in his hydrodynamic model on the basis that its contribution is small relative to the evaporation rate.

Nevertheless, a significant shift in the appreciation that SGD to the Coorong lagoons could be an important contributing factor to the hydrology, salinity and nutrient status of the lagoons has evolved over a number of studies. Significant among these was the work of (Chris *et al.* 1975) and (Haese *et al.* 2008) who constructed a generalised cross–

section of the Coorong area showing how seawater regimes and groundwater from the West could merge and drive water upwards into the Coorong lagoons (Figure 3). Initial investigations under CSIRO's flagship for a Healthy Country, involving CSIRO, Adelaide University, Flinders University, The South Australian Research and Development Institute and Geoscience Australia, led them to believe that submarine ground water discharge into the Coorong could be a potential primary control on water quality of the lagoons. In response to their conviction a study was conducted by (Haese *et al.* 2008) which employed remote sensing studies - using thermal based classification of Landsat 5 TM imagery (Figure 4) and field observations to identify submarine groundwater discharge as a major process contributing to water quality within the Coorong.

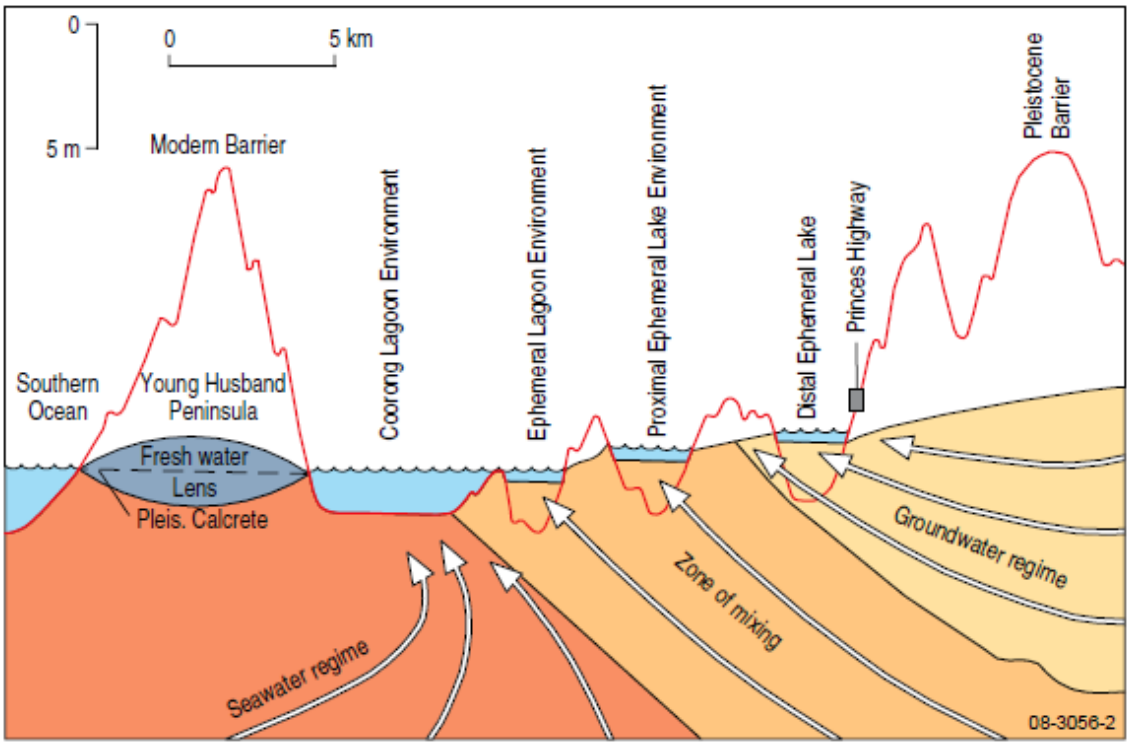

Figure 3: A generalized cross section of the Coorong with associated Ephemeral Lakes illustrating the zone of mixing between the groundwater and seawater regime of subsurface flows. Taken from (Haese *et al.* 2008) as modified from (Chris *et al.* 1975).

Figure 4: Landsat 5 TM based thermal classification of the Coorong and Lower Lakes region. Red indicates groundwater discharge zones classified by spectral imagery. Figure taken from (Haese *et al.* 2008).

2.4 Isotope tracing of groundwater inputs using Strontium (Sr)

With the advent of improved technology, the analysis of isotopic ratios of major cations such as strontium has allowed for tracing of various endmember water inputs into mixed sourced bodies (Capo *et al.* 1998). Furthermore, the use of these isotopic ratios along with mass balance equations allows the prediction of the contribution from each of the endmembers to the elemental concentrations of the water body. In turn, with elemental concentration data the relative mass inputs of these water sources can be calculated (Holmden *et al.* 2012). Strontium isotopes were selected for the purpose of this study as strontium has been shown in a prior study by *Gillanders et. al. (2012)* to be conservative with salinity even in the hypersaline South Lagoon and thus would allow groundwater contributions to be determined within these waters.

2.5 Strontium isotope abundance and isotopic ratios

In order of mass number the four stable isotopes of Strontium are ^{84}Sr, ^{86}Sr, ^{87}Sr, and ^{88}Sr. Of the four stable isotopes ^{84}Sr, ^{86}Sr, and ^{88}Sr have a fixed abundance and thus their percentage ratios remain fixed. ^{87}Sr abundance increases over time as a result of beta minus decay of Rubidium 87 (^{87}Rb) with a half-life of 4.92×10^{10} years. Although only slightly radioactive because of its long half-life, the production of radiogenic strontium 87 is significant as rubidium is relatively abundant, and 28% of it is in its radioactive form (Butterman & Reese Jr 2003). Consequently, Strontium 87 either originates from the primordial material that formed the Solar system or from radiogenic decay of rubidium. It is the relative amounts of primordial strontium to radiogenic strontium that permits for the differential measurements of isotope ratios as they occur in the source material being investigated. The most commonly used isotope ratio is that of ^{87}Sr to ^{86}Sr expressed as $^{87}Sr/^{86}Sr$.

2.6 Variations in radiogenic strontium isotopes ($^{87}Sr/^{86}Sr$) in the Coorong

Both the North and South lagoons of the Coorong have many well defined areas that have extensive carbonate deposits (Haese *et al.* 2008). One visibly obvious manifestation of carbonate deposition are the tufa: these circular limestone structures resemble small spent and hollowed out cinder cone volcanoes that can reach cross-sectional diameters of up to 1m. Tufa in the Coorong are largely the result of calcium precipitation that has occurred by groundwater discharge. Haese et al. (2008) noted that the distinct concentric carbonate laminations suggest a cyclic accretion process. Incorporation of calcium, into tufa has been strongly associated with microbial induced precipitation (Ford & Pedley 1996, Smith *et al.* 2004, Pedley *et al.* 2009).

The ability of strontium to substitute for calcium is well documented (Budd *et al.* 2000, Hoppe *et al.* 2003, Horstwood *et al.* 2008). Strontium deposition into tufa has been demonstrated by (Li *et al.* 2008) in Southern California's Salton Basin; and by (Benson & Peterman 1996) in a sub-basin in Pyramid Lake Nevada, however both studies noted that there was no conclusive evidence for the fractionation of strontium isotopes. Li et al. (2008) also noted that because the residence time of strontium in the lake was relatively short (typically 3-4 years) any fractionation that might have occurred would be insignificant in altering the isotopic ratios of strontium in the lake basin. Extending the same rationale of short residence time to the Coorong is problematic, none the least because it is a reverse estuary. However, as barrage flows, carrying relatively low salt loads, in recent times have been relatively normal, it can be assumed that water mixing throughout the Northern lagoon at least will have been sufficient to negate any significant alteration of $^{87}Sr/^{86}Sr$ ratios due to any possible fractionation into the carbonate deposits and tufa, if it occurs at all to an appreciable extent. Furthermore, as

$^{87}Sr/^{86}Sr$ values are normalised to the constant value $^{86}Sr/^{88}Sr$ 0.1194 in mass spectrometer analysis, any radiogenic strontium isotope values will be unaffected as any small amount of fractionation in $^{87}Sr/^{86}Sr$ is corrected (Steiger & Jäger 1977). The increased resolution of mass spectrometers permits the $^{87}Sr/^{86}Sr$ ratio to yield information of the strontium source, and the $^{88}Sr/^{86}Sr$ ratio, the amount of mass dependent fractionation that the source has experienced.

2.7 Strontium inputs into the Coorong

For the present study the main strontium sources and isotopic ratios that require primary consideration are (i) coastal Southern Ocean seawater proximal to the Coorong; and (ii) local Submarine Groundwater Discharge. Of lesser direct importance are the strontium loads carried by (iii) barrage release water from the Murray River and the lower Lakes Alexandrina and Albert; (iv) water that enters the Coorong through the Upper South Eastern Drainage System (USEDS); and (v) local precipitation. These former are briefly considered below in terms of their measured or estimated concentrations and isotopic ratios in context of previous findings.

2.7.1 STRONTIUM ISOTOPES IN SEAWATER

The concentration of strontium and its isotopic ratios in seawater, along with several other standards, have provided researchers an invaluable tool with which to reconstruct much of the oceans paleo record (Richter & DePaolo 1988, Richter & Liang 1993). Through the processes of weathering, radioactive rubidium and its decay product, radiogenic strontium is constantly increasing the net balance of strontium in the bulk silicate Earth and consequently, during times of more intense weathering of silicates the oceans become more radiogenic in terms of $^{87}Sr/^{86}Sr$ (Singh *et al.* 1998). Examination

of the strontium isotopic $^{87}Sr/^{86}Sr$ ratios in the marine carbonate deposits has enabled researchers to make estimates of past climate events by constraining changes in the riverine influx of strontium and other solutes through time from weathering of continental rocks (Richter & DePaolo 1988, Richter & Liang 1993).

For a long time oceanic strontium levels were believed to be between 8.0 and 8.2 ppm; however Angio et. al., (1966) on the basis of 91 samplings of five widely separated areas of the North Atlantic Ocean, and using both deep water and surface samples, suggested that a more correct value for oceanic strontium would be between 7.2 and 7.8 ppm. Because strontium has a relatively long residence time of approximately 2.4Myr (Viezer 1989), and because oceanic mixing occurs over every 1000 years, strontium concentrations and its isotopes are distributed homogenously (Hess *et al.* 1986). Spatial and temporal variations in both the strontium concentration and the isotopic $^{87}Sr/^{86}Sr$ ratio may vary near coastlines and offshore due to inputs of more radiogenic ^{87}Sr from continents by rivers or carried by dust particles (Pearce *et al.* 2015).

In terms of isotopic $^{87}Sr/^{86}Sr$ ratios present day seawater is globally homogenous at approximately 0.709172 (Richter *et al.* 1992, Capo *et al.* 1998). This isotopic concentration is reflected in all oceanic calciferous deposits that have been formed both by organic and inorganic processes in recent times (Hess *et al.* 1986).

2.7.2 STRONTIUM ISOTOPES IN GROUNDWATER

Strontium isotopes can be valuable in outlining the movement of water through aquifers and help identify areas where various aquifers with distinct $^{87}Sr/^{86}Sr$ ratios merge, and discharge (Raiber *et al.* 2009). However, due to the complexity of many groundwater sources there is usually a need to use several isotopic tracers and / or rare elements to help determine provenance with greater resolution. (Shand *et al.* 2009). Strontium

isotopic data of groundwater located in the upper Murray-Darling basin have been collected (Raiber *et al.* 2009); however, strontium data for the lower reaches of the Murray River and the Lower Lakes is not as abundant. Strontium concentrations in groundwater have been recorded with significant variation dependant on the host rock it passes through, a study by (Skougstadt & Horr 1960) which measured over 150 samples of groundwater across the US reported concentrations ranging 0.2 – 36 ppm and groundwater to carry a significantly higher radiogenic signature of ^{87}Sr compared to modern seawater.

2.7.3 STRONTIUM ISOTOPES IN RIVERS

The rate of strontium input into rivers is largely determined by the intensity of weathering reactions and the type of substrate that is being eroded (Palmer & Edmond 1992). In terms of weathering dynamics, it is the large scale geological events such as glaciation events and continental collisions that liberate radiogenic ^{87}Sr in great quantities (Capo *et al.* 1998). Limestone and chemically precipitated sediments (evaporites) and silicate rocks are the main contributors to the increase in strontium to the oceans via river inputs (Capo *et al.* 1998). The global average $^{87}Sr/^{86}Sr$ ratio for riverine water is placed at 0.7119 and strontium concentration at <1 ppm (Wang *et al.* 2007).

2.7.4 STRONTIUM ISOTOPES IN PRECIPITATION

Far from being a pure condensate of water vapour, rainwater plays a major role in the transfer of elements, compounds, and products of weathering to hydrological catchments and soils. Analysis of isotopic ratios of strontium in rainwater has increased the ability of researchers to trace the provenance of the water vapour and consequent

precipitation from its sources. If for instance the rainwater carries a high radiogenic signature of strontium than provenance is a likely to have a terrestrial origin (Pearce *et al.* 2015). Studies by Miller et. al. (1993), Gaustein and Armstrong (1983), Gosz et al. (1983), Aberg et al. (1989) and Herut et al. 1993 place the concentration range of strontium in precipitation extremely low, ranging just 0.0007 – 0.383 ppm and hence will not produce any significant shift in $^{87}Sr/^{86}Sr$ values within the lagoons even if it were to be substantially more radiogenic than the groundwater / seawater. $^{87}Sr/^{86}Sr$ values reflect the source they were evaporated from due to the inability of strontium to fractionate in precipitation because of the low mass differences between its isotopes.

3. METHODS

3.1 Sampling and storage

Samples of water were collected along the length of the Coorong system and other adjacent water bodies (Figure 1) on two separate dates (

Table 1) in acid washed polypropylene bottles. The Southern lagoon was sampled on April 10th, 2015 and the Northern lagoon on May 15th, 2015 with samples collected at Robs Point in the south part of the Northern lagoon on each trip for reference. Samples of each end member water reservoir (Murray River, Southern Ocean, and Local Groundwater) were also taken to allow for analysis and later source discrimination in the lagoonal samples. Whenever possible, water was sampled at a depth approximately midway between the lagoon floor and the water's surface (on average ~1m depth) at a

point approximately in the middle of that particular part of the lagoon however due to the varying nature of the lagoons this was not always achievable. Water in the South of the Southern lagoon was mostly very shallow (<0.5 m). Sampling in the Northern lagoon was conducted by two teams, with the southern part of the Northern lagoon being explored / sampled via car and wading into the water to collect and the northern part being sampled from a small boat. Sample collection within the southern part of the Northern lagoon was restricted by road access and land ownership, whereas sample collection from the boat was much more evenly distributed, however due to the deeper nature of this section and the samples being collected from the boat, the samples were not collected at a depth approximately midway between the lagoon floor and water's surface but at a depth reachable from the vessel (~ 1m) from the water's surface. Furthermore at a point in the South lagoon midway between Parnka Point and Woods Well, a large abundance of tufa in a circular deposit which trapped water within it with almost no connectivity to the lagoon it was residing in was sampled along with nearby lagoon waters to test for active groundwater discharge occurring within the tufa (Figure 5). Samples of groundwater were taken from two separate wells located 800m apart near Noonameena (Figure 1) on a separate occasion from the North and South lagoons once field observations and initial measurements had confirmed active SGD in the region. To minimize the contribution of recent precipitation, the pH, salinity, conductivity and total dissolved solids of the water were measured regularly as the wells were pumped and samples were collected only once these parameters stabilized. GPS coordinates were recorded for each sample. The samples were labelled upon collection and sealed air tight using parafilm. Upon returning from the field samples were stored refrigerated at 4.0^{o}C.

Figure 5: Satellite imagery showing sampling locations within the South lagoon approximately mid-way between Parnka Point and Woods Well. The red boundary highlights a body of water trapped within a highly abundant circular deposit of large tufa which was observed in the field and is easily distinguishable from satellite imagery on Google Earth. Pins indicate sampling locations and sample IDs.

3.2 Filtration of samples

Each sample was filtered the day following collection using a 0.45µm polycarbonate filter to remove particulate matter allowing for analysis of just the dissolved component of Sr (Capo *et al.* 1998) and avoid complications with solution ICP-MS and TIMS analysis. The filtered water was stored in an acid washed 50mL polypropylene test tube and kept sealed and refrigerated at 4.0^{o}C. A large portion of each original sample was retained, resealed, and stored in the refrigerator for stock and potential future analyses.

All samples were probed for pH, conductivity, salinity and total dissolved solids (TDS) using a Hanna Instruments HI-98194 multiparameter meter. Prior to conducting the measurements the multimeter was calibrated for pH and conductivity using standard

solutions with known pH, conductivity and salinity. Samples were each poured into a clean polycarbonate testing vial which had been thoroughly rinsed with deionized water beforehand. Both the testing vial and the probes on the multimeter were thoroughly rinsed with deionised water between measurements to avoid cross contamination of the samples. After every ten samples measured, pH and conductivity of a test standard for each parameter with an approximately equal magnitude to that of the field samples was tested with the multimeter to ensure that no instrument drift was occurring.

Salinity levels above 70 PSU were above the measureable limit of the instrument and hence were unable to be recorded directly. Consequently these samples with a salinity >70 PSU were diluted to a 1:5 ratio by mixing 20mL of the sample with 80mL of deionised water. The diluted samples were re-probed for conductivity and salinity and the measured values were multiplied by a factor of five to give the true values of the samples conductivity and salinity.

The instrument is specified to have the following accuracies for the following parameters;

pH	± 0.02 pH
Conductivity	± 1% of reading OR ± 1 μS/cm (whichever is greater)
Salinity	± 2% of reading OR ± 0.01 PSU (whichever is greater)
TDS	± 1% of reading OR ± 1ppm (whichever is greater)

Dilution of samples with salinities >70.00 PSU introduces additional error estimated to be ± 5%.

3.3 Solution ICP-MS for elemental concentrations of Na, Sr and Ca

Inductively Coupled Mass Spectometry (ICP-MS) was conducted at Adelaide Microscopy using an Argilent 7500cs to obtain elemental concentrations of Na, Sr and Ca. Analysis was run with an Octopole Reaction System (ORS), allowing the removal of interfering signals and hence better accuracy, by bleeding helium gas into the path of the ions. As the detection limit of the solution ICP-MS machine sits between 10 – 500ppb, lagoon water samples had to be diluted to sit within this range to and obtain accurate results. The dilution factor required for each sample to sit within the detection limit was estimated from established global seawater averages of elemental concentrations coupled with measurements of the samples salinity. Samples were diluted using 2% ultrapure HNO_3 with a pipette using acid washed tips. The mass of each sample was measured before and after dilution with the nitric acid to allow the best possible accuracy when correcting results with the dilution factor. Blanks and standards were prepared using the same method and were procedurally analysed between sample sets to allow calibration of the resultant data. Resultant data was readjusted to the true concentrations of the samples by multiplying them back by their dilution factors.

3.4 Thermal Ionization Mass Spectrometry (TIMS) Analysis

3.4.1 PREPARATION OF TEFLON VIALS FOR SAMPLE EVAPORATION

Cleaning of 10mL round bottomed Teflon vials was conducted in a clean laboratory to avoid any contamination entering the vials as strontium is ubiquitous in nature (Capo *et al.* 1998, Stewart *et al.* 1998). Furthermore as the sample sizes to be collected in the vials for TIMS analysis were ~1µg, samples are very easily contaminated by only a minute amount of foreign material.

3.4.2 GRAVITY FLOW CATION-EXCHANGE CHROMATOGRAPHY

Using concentration data from solution ICP-MS, a volume of filtered sample water containing ~1000ng (1μg) of Sr was calculated for each selected sample and evaporated in an acid washed Teflon vial at 50^{o}C to avoid any potential high temperature reactions within the sample.

Acid washed, Teflon, strontium-spec, cation exchange columns were rinsed through three times with DI water and injected with 2000μL SrSpec© resin to the neck of the column using a 1000μL pipette, ensuring no bubbles formed inside. The columns were then washed through with a reservoir of 3.5M HNO_3, followed by two reservoirs of DI water and then conditioned with 0.5mL, 3.5M HNO_3. The evaporated samples were dissolved in 0.5mL of 3.5M HNO_3 and loaded into the neck of the columns carefully to avoid forming any bubbles or perturbing the resin by using a 1000μL pipette. Four discrete volumes of 0.3mL 3.5M HNO_3 were washed through the columns to elude unwanted metal cations of Cu, Mg, Zn, Fe and Cd. Once all of the HNO_3 had passed through the column, prepared acid washed 10mL Teflon vials were placed underneath the Sr-spec columns and two discrete 0.5mL volumes of DI water were used to rinse the strontium attached to cation exchange sites on the SrSpec© resin into the vials, dissolved in the DI water. The samples were then evaporated to be ready for isotopic analysis.

3.4.3 MASS SPECTROMETRY FOR ISOTOPIC RATIOS $^{87}SR/^{86}SR$

The separated strontium samples from cation exchange chromatography were redissolved in 1μL of 'Birck's loading solution' so that the concentration of Sr in solution was ~1μg /μL. The redissolved samples were loaded onto outgassed, zone-

refined rhenium filaments using a 1μL pipette with acid washed tips and were evaporated using an electric current to heat the filaments.

Analysis of the Sr isotopic ($^{87}Sr/^{86}Sr$) composition was performed using a Phoenix Isotopix Thermal Ionization Mass Spectrometer (TIMS) using traditional Sr analysis methods such as described by (Capo *et al.* 1998). Mass dependant fractionation from instrumental analysis of samples was corrected for by normalization of non-radiogenic $^{86}Sr/^{88}Sr$ to a value of 0.1194. Routine measurements of known standards of NIST987 ensured results obtained were reproducible with 2 standard deviations totalling <0.000030.

3.5 Strontium isotope mass balance equations

By utilizing Strontium isotope data of $^{87}Sr/^{86}Sr$ obtained by TIMS analysis, the fractional input of Sr into the lagoons from groundwater was calculated with the use of simplified bimodal mixing equations as described by (Capo *et al.* 1998, Holmden *et al.* 2012) (

Equation 1, 2 and 3). End members for Sr input into the lagoons were assumed to be (i) coastal Southern Ocean seawater and (ii) local fresh groundwater discharge after logistical analysis of potential endmember configurations showed this to the best explanation for observed values.

Equations 1,2 and 3 to describe isotopic and volume mass balance are provided below where the following subscripts are used;

- Sample = Lagoon water sample
- SW = Seawater from the Southern Ocean
- GW = Groundwater collected from Noonameena

Equation 1: Isotopic mass balance of strontium

$$\frac{^{87}Sr}{^{86}Sr}_{Sample} = \frac{^{87}Sr}{^{86}Sr}_{SW} * F_{SW} + \frac{^{87}Sr}{^{86}Sr}_{GW} * (F_{SW} - 1) \quad \textbf{(1)}$$

Where;

F_{SW} is the fractional input of SW to the lagoons

Equation 2: Bimodal mixing equation for Sr input from GW into lagoons

$$F_{GW}^{Sr} = \frac{\frac{^{87}Sr}{^{86}Sr}_{Sample} - \frac{^{87}Sr}{^{86}Sr}_{SW}}{\frac{^{87}Sr}{^{86}Sr}_{GW} - \frac{^{87}Sr}{^{86}Sr}_{SW}} \quad \textbf{(2)}$$

Where;

F_{GW}^{Sr} is the fraction of Sr in the Coorong waters originating from SGD

Equation 3: Bimodal mixing equation for relative mass contribution of GW to the lagoons

$$F_{GW}^{Mass} = \frac{[Sr]_{SW} * (\frac{^{87}Sr}{^{86}Sr}_{SW} - \frac{^{87}Sr}{^{86}Sr}_{Sample})}{[Sr]_{GW} * (\frac{^{87}Sr}{^{86}Sr}_{Sample} - \frac{^{87}Sr}{^{86}Sr}_{GW}) + [Sr]_{SW} * (\frac{^{87}Sr}{^{86}Sr}_{SW} - \frac{^{87}Sr}{^{86}Sr}_{Sample})} \quad \textbf{(3)}$$

Where;

F_{GW}^{Mass} is the fraction of the mass of water originating from the SGD

Quantitative determination of the input of each endmember was achievable due to each endmember possessing a characteristic isotopic ratio of $^{87}Sr/^{86}Sr$.

4. OBSERVATIONS AND RESULTS

4.1 Salinity and Elemental Concentrations vs. Latitude of the Coorong Lagoon waters.

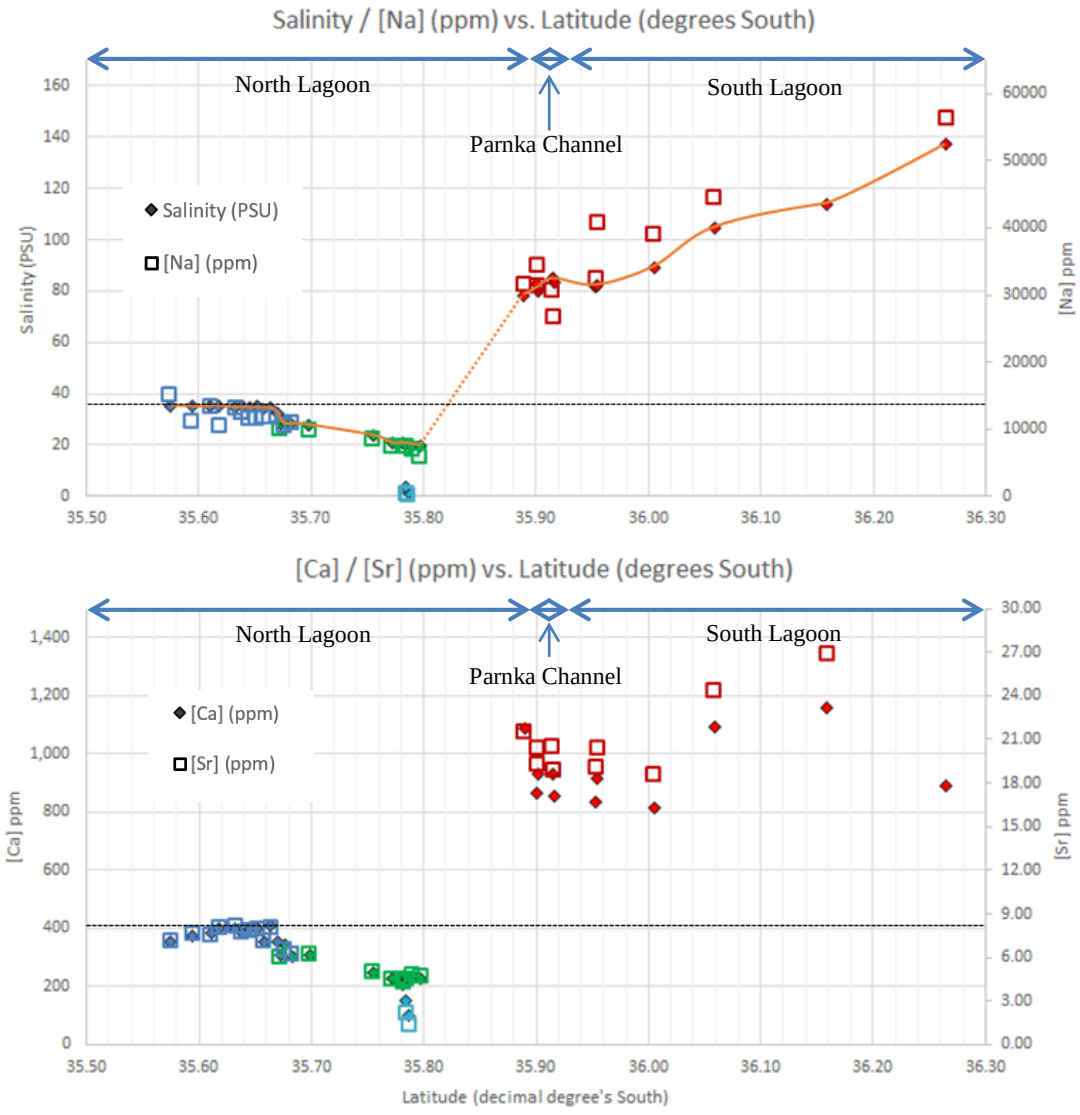

Figure 6: Plots of (a) salinity & Na concentration and (b) Ca & Sr concentrations of the Coorong lagoon waters vs. latitude in decimal degrees South. All variables indicate a dilution of seawater in the southern end of the Northern Lagoon by some additional, fresher water source. Lagoon water samples were taken on two separate dates with a common reference site sampled on each date. Groundwater samples (plotted in light blue) were collected on a later date from two separate wells near Noonameena once initial results confirmed some freshwater input in the vicinity. In plot (a) the dashed black line indicates the measured salinity of Southern Ocean seawater, the orange line shows the general trend in salinity of the Coorong lagoons. A zoom of each plot (a) and (b) showing North Lagoon waters only are given below to better illustrate the measured decreasing salinity trend.

4.2 Salinity and Elemental Concentrations vs. Latitude of the North Lagoon

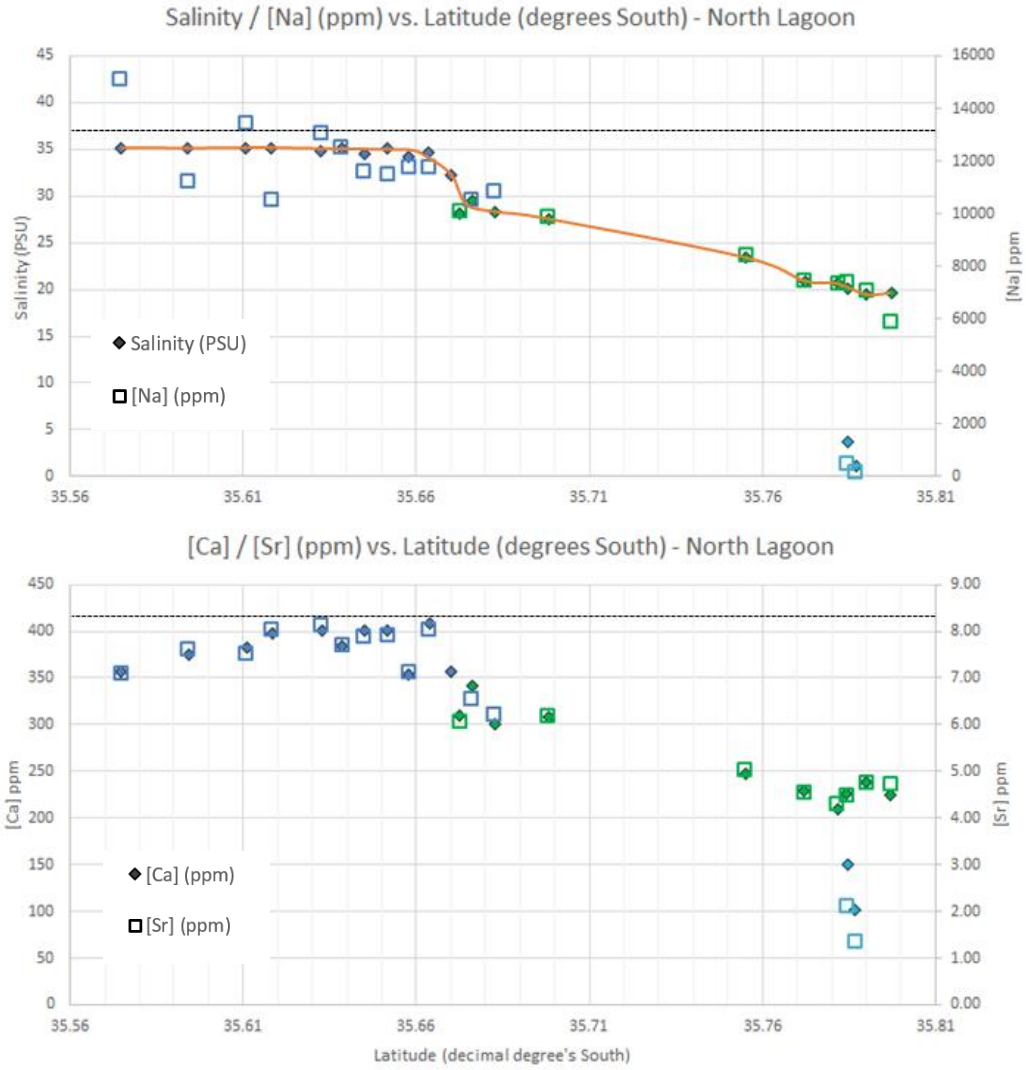

Figure 7: Plots of (a) salinity & Na concentration and (b) Ca & Sr concentrations of the North Lagoon waters of the Coorong vs. latitude in decimal degrees south. All variables indicate a dilution of seawater in the southern end of the Northern Lagoon by some additional, fresher water source between 35.66 – 35.81 decimal degrees south latitude. In plot (a) the dashed black line indicates the measured salinity of Southern Ocean seawater; the orange line shows the general trend in salinity of the North lagoon. In plot (b) the dashed black line illustrates measured Southern Ocean seawater values of Ca and Sr concentrations.

Table 2: Correlation coefficients between elemental concentrations and salinity

Parameters	Relationship	Equation	Correlation Coefficient (R^2)
[Na] (ppm) vs. Salinity (PSU)	Linear	408.64x-1205	0.9759
[Sr] (ppm) vs. Salinity (PSU)	Linear	0.236x-0.0946	0.9861
[Ca] (ppm) vs. Salinity (PSU)	Linear	10.322x+28.313	0.9722

4.3 North Lagoon and Lower Lake water as a product of mixing between different endmembers

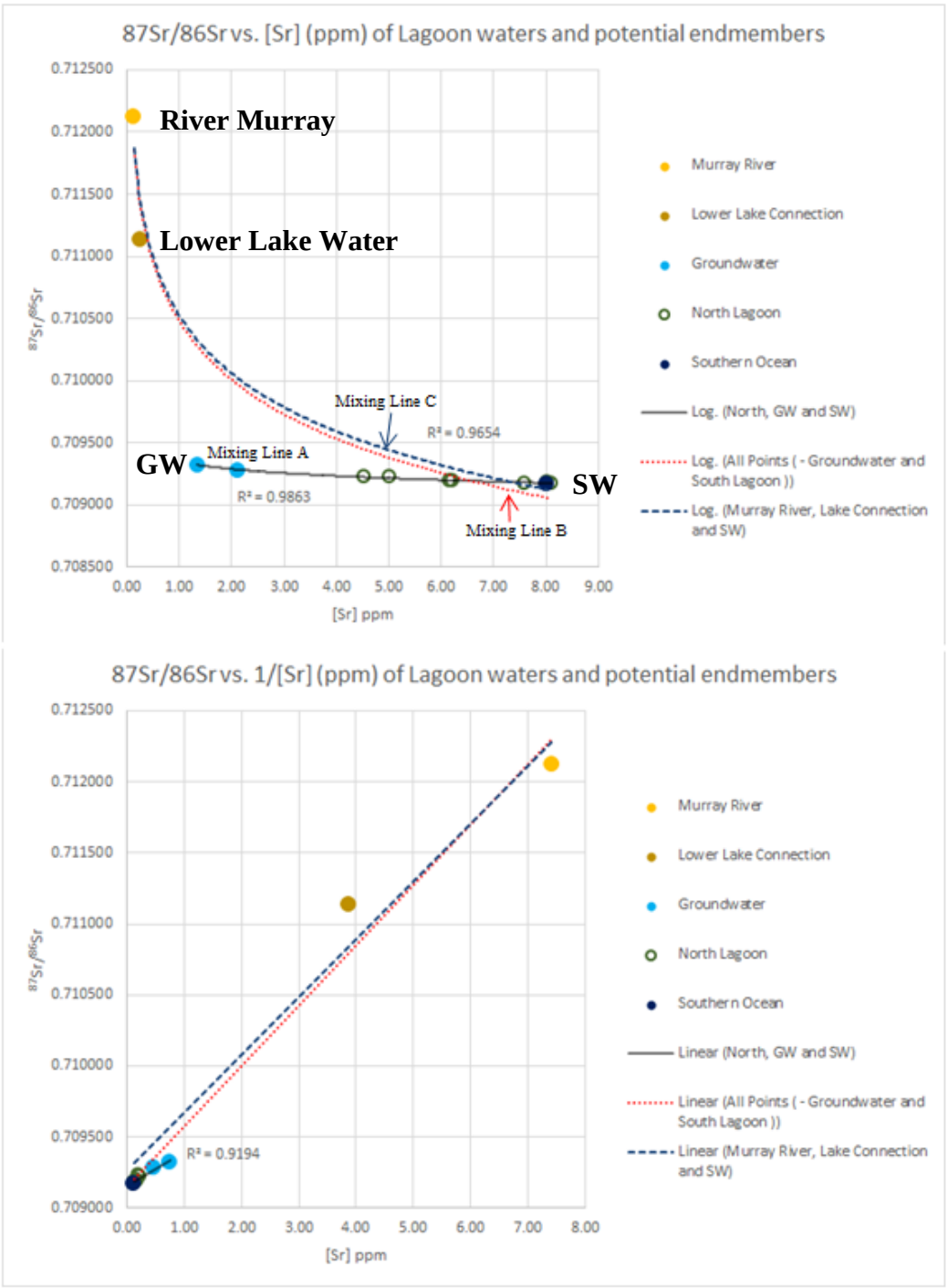

Figure 8: (a) Hyperbolas formed by the mixing of different potential endmember components with characteristically different Sr concentrations [Sr] and radiogenic strontium isotopic ratios ($^{87}Sr/^{86}Sr$) within the Coorong's North Lagoon. (b) Plot of the $^{87}Sr/^{86}Sr$ of the samples against the reciprocal of the Sr concentration (1/[Sr]). Plotting the reciprocals of the concentrations transforms mixing hyperbola into straight lines; if the hyperbola curves are related to some fractionation process which is an exponential relationship, plotting the isotopic ratio against the reciprocal of concentration would not produce linear tends (Faure 1977, Kendall & McDonnell 2012).

4.4 North Lagoon water as a product of mixing between SGD and seawater

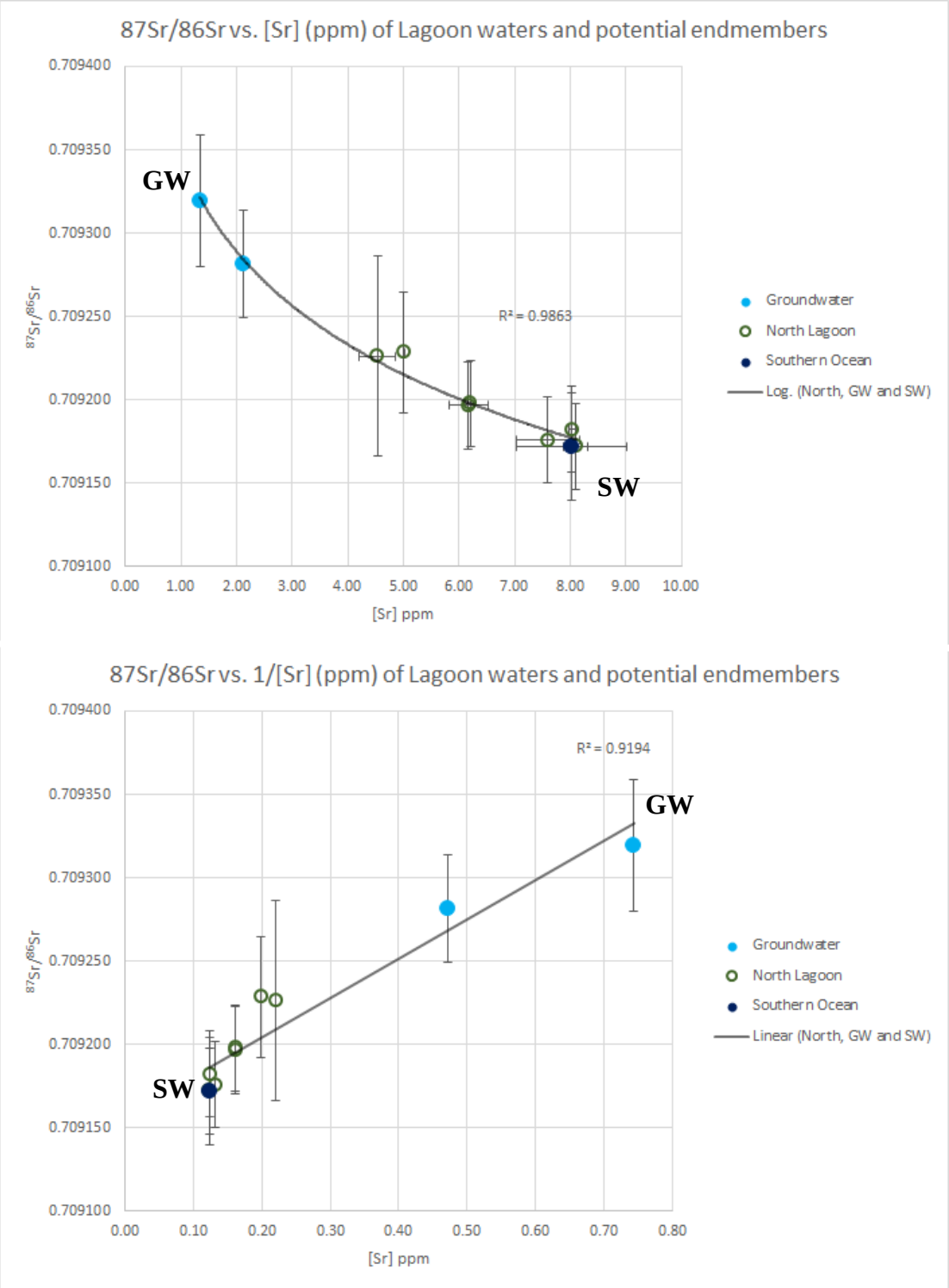

Figure 9: (a) Hyperbolic mixing curve between endmembers of groundwater and seawater with characteristically different Sr concentrations [Sr] and radiogenic strontium isotope ratios ($^{87}Sr/^{86}Sr$). (b) Linear mixing line produced by plotting the $^{87}Sr/^{86}Sr$ values against the reciprocal of the Sr concentration (1/[Sr]).

4.5 Calculated contributions of groundwater to the strontium budget of the lagoons and the relative mass of groundwater required to explain these values

Table 3: Table of $^{87}Sr/^{86}Sr$ values and the calculated fraction of Sr input from groundwater discharge to account for the measured $^{87}Sr/^{86}Sr$ of the samples. Fractional input of Sr calculated using simple bimodal mixing equation (

Equation 1)

Sample ID	^{87}Sr / ^{86}Sr	2x RSD.	[Sr] (ppm)	2x RSD.	F_{GW}^{Sr} (Equation 1 2)	F_{GW}^{Sr} (As %)	F_{GW}^{Mass} (Eq 3)	F_{GW}^{Mass} (As %)
Lagoon waters								
SL1B	0.70923809	0.000030	19.31	0.850	0.45	45	0.85	85
SL2	0.70924123	0.000034	21.52	1.027	0.47	47	0.87	87
SL4A	0.70924444	0.000030	20.48	1.552	0.49	49	0.88	88
NL6	0.70922615	0.000060	4.54	0.323	0.37	37	0.78	78
NL7	0.70922848	0.000036	5.01	0.015	0.38	38	0.80	80
NLB1	0.70919668	0.000026	6.17	0.348	0.17	17	0.52	52
NLB3	0.70919774	0.000026	6.20	0.077	0.17	17	0.54	54
NLB6	0.70918231	0.000026	8.04	0.064	0.07	7	0.28	28
NLB11	0.70917212	0.000026	8.11	0.220	0.00	0	0.00	0
NLB15	0.70917591	0.000026	7.60	0.564	0.03	3	0.12	12
End Members								
JWP2	0.709319347	0.000039	1.34	0.020	1.00	100	1.00	100
BWP2	0.70928140	0.000032	2.12	0.004	0.74	74	0.95	95
SW	0.70917203	0.000032	8.02	0.011	0.00	0	0.00	0
Other Samples								
LL3	0.711134	0.000028	0.26	0.009	-	-	-	-
MR1	0.712124	0.000026	0.13	0.008	-	-	-	-
SL3	0.70926617	0.000026	44.40	3.212	0.64	64	0.91	91

5. DISCUSSION

5.1 Salinity vs. Latitude

Likewise to former studies as mentioned prior such as those by (Commission 2006, Brookes *et al.* 2009, Krull *et al.* 2009), measurements of salinity across the Coorong lagoons showed a salinity gradient increasing from near marine levels in the Northern reaches of the North Lagoon to hypersaline conditions with >3 times seawater salinity in the Southern end of the South lagoon (Figure 6). Unlike these former studies however results of this study found salinity levels to first decrease in the Southern end of the North Lagoon detectable between Mark Point and Robs Point before sharply increasing to hypersaline conditions >70PSU within Parnka Point Channel and further increasing to the South throughout the South Lagoon and reaching >130PSU at the tail end. It's important to note that the reference point at Rob's Point yielded near marine salinity (34.45PSU) on the first sampling date (April, 10th) and nearly half marine salinity (19.69PSU) on the second sampling date (May, 15th). This suggests that groundwater discharge can have profound effects on the salinity levels of the Coorong however these effects are likely temporal and may be related to other natural phenomena such as periods of high recharge of the groundwater aquifer of interest. Furthermore as access was restricted between Rob's point and Parnka Point no samples were able to be collected throughout and thus the salinity gradient was extrapolated in this region hence the true nature of salinity in this region is poorly defined by this study. It is also important to note that as the South Lagoon samples were collected on a separate date to the North Lagoon samples, the former being when the groundwater discharge was detected, that the salinity gradient across the lagoons may not have been as steep if

sampling was conducted within a tighter timeframe and if groundwater discharge detected during sampling of the North Lagoon was pervasive through Parnka Point Channel and along the reach of the South Lagoon.

5.2 Elemental Concentrations vs. Latitude

Elemental concentration data of Sodium (Na), Strontium (Sr) and Calcium (Ca) were obtained by solution ICP-MS for the purpose of supporting salinity measurements across the lagoons to evidence groundwater discharge as they have been shown to be conservative with salinity of the Coorong lagoons by *Gillanders et. al. (2012)*. This conservative behaviour has been evidenced in this study (See Figure 6 Figure 7 and Table 2 of correlation coefficients). Although there is some degree of deviation from the linear trend of concentration vs. salinity in the concentrations of Sr and Ca in hypersaline waters associated with dissolution and precipitation of minerals such as calcium carbonates, the studies by *Gillanders, et. al. (2012)* determined the degree of such to be low enough to neglect it for the purpose of supporting salinity data.

As lagoon samples had to be diluted by a factor of ~100,000 times to be within the detectable limits of the ICP-MS for measuring Na concentration, there was additional error introduced by series dilutions estimated to be ~ ±5%, however results were still sufficient for supporting salinity data. As can be seen in Figure 6 and Figure 7, trends for concentration of each element vs. latitude closely match that of salinity vs. latitude, further evidencing groundwater discharge between Mark Point and Noonameena.

5.3 Estimates of potential freshwater contributors to observed salinity decrease

The initial decrease in salinity from North to South between Mark Point and Rob's Point was determined to be dominantly related to fresh groundwater discharge after analysis and consideration of all other potential fresh water endmembers including; (i) barrage release water from the Murray River and the lower Lakes Alexandrina and Albert, (ii) water that enters the Coorong through the Upper South Eastern Drainage System (USEDS) and (iii) local precipitation. A scrutiny of why each of these endmembers has been disregarded as a significant contributor to this initial decrease in salinity is provided below.

5.3.1 BARRAGE RELEASE WATER FROM THE MURRAY RIVER AND THE LOWER LAKES ALEXANDRINA AND ALBERT

Although water from the River Murray residing within the Lower Lakes constitutes the largest proximal fresh water body to the Coorong lagoons, it is not logistically sensible from data obtained during this study that the observed negative trend in salinity could be caused by barrage fluxes. If discharge of this water through the barrages was responsible for the observed salinity decrease than we would expect to see the greatest decrease in salinity adjacent the barrages between Lower Boundary Creek and Mark Point. We instead however see the greatest decrease from marine salinity values in the North Lagoon occurring >25km South from the most southern barrage, between Noonameena and Robs Point. Salinity and elemental concentrations of Na, Ca and Sr retain near marine values adjacent the barrages.

5.3.2 WATER FROM UPPER SOUTH EAST DRAINAGE SCHEME (USEDS)

Discharge from the USEDS occurs at the tail end of the South Lagoon near Salt Creek. This freshwater discharge is unable to explain the observed salinity decrease within the North Lagoon as it would first mix with hypersaline waters of the South Lagoon and thus could not be responsible for reducing North Lagoon waters to below marine values.

5.3.3 LOCAL PRECIPITATION

Precipitation would be expected to see a more homogenous dilution of salinity and elemental concentrations across the North Lagoon. Water depth would have a localized control on the degree of dilution caused by precipitation, however we would not see such a steep decline in salinity ranging from latitudes 35.66 – 35.69 degrees (See Figure 7) where water depth is approximately equal. As there was no local precipitation during the day of sampling it can be assumed that effective mixing of the North lagoon waters as explained by Webster et. al. (2008) would eliminate the possibility that this steep decline reflects the residual gradient of a precipitation front.

5.4 Lagoon waters as product of mixing between groundwater and seawater

5.4.1 TWO COMPONENT MIXING HYPERBOLA

As explained by (Faure 1977) plotting isotopic compositions against their concentrations is a powerful tool for visually determining if samples can be explained as a mixing product of two endmember sources. Such plots will not necessarily produce straight lines but instead will produce hyperbolic curves, unless there is no difference in elemental concentration of the endmembers in which case a straight line will be produced. Furthermore if the samples can be explained as a mixing of two endmember

sources, than plotting the isotopic compositions against the reciprocal of the elemental concentration (1/concentration) should produce a linear relationship.

Figure 8a shows hyperbolic mixing trends of three different endmembers (seawater, groundwater and river water) to explain the isotopic $^{87}Sr/^{86}Sr$ values of the North Lagoon waters of the Coorong and Lower Lakes including;

- Mixing line A: North Lagoon samples as a mixing product of fresh submarine groundwater discharge with Southern Ocean seawater

- Mixing line B: Lower Lake water as a mixing product of River Murray water with Southern Ocean seawater. Note that a strong trend cannot be confirmed by results of this study as only one measurement of $^{87}Sr/^{86}Sr$ was taken for the Lower Lakes, as it was not a major focus of this study.

- Mixing Line C: North Lagoon samples as a mixing product of Lower Lake water discharging through the barrages and of groundwater with Southern Ocean seawater.

It can be seen by these plots that North Lagoon samples are best explained by ‘mixing line A’ as a mixing product of fresh submarine groundwater discharge with Southern Ocean seawater. Although North Lagoon samples can mostly be explained by mixing line C of Lower Lake water with Seawater within the error margins, the correlation is not as strong as mixing line A and as previously indicated is logistically insensible according to the decline in salinity away from the barrages.

Figure 9a displays the mixing hyperbola formed with groundwater and seawater exclusively and includes vertical and horizontal error bars of 2 standard deviations to give better visualisation of mixing line A. All samples of the North Lagoon sit along the hyperbolic curve within the error margins supporting the contention that the North Lagoon waters are the product of mixing between fresh groundwater and Southern Ocean seawater.

5.4.2 LINEAR TRANSFORMS OF HYPERBOLIC MIXING CURVES

Linear transforms of the hyperbolic mixing curves formed by instead plotting $^{87}Sr/^{86}Sr$ against 1/[Sr] enable further that the samples can be explained by a simple mixing product of the assumed two endmembers. Referring to mixing line C in Figure 8b, it can be further confirmed that mixing of Lower Lake water with Seawater to explain the North Lagoon samples is not viable as samples and endmembers do not show a strong conformity to the produced linear relationship. Mixing line A however assuming endmembers of fresh groundwater and seawater to explain North Lagoon samples shows all samples conforming to the produced mixing line within their error margins of 2 standard deviations (see Figure 9b) further supporting the theory that North Lagoon waters can be explained as a product of mixing of these two sources.

5.5 Quantifying the contribution of strontium to the lagoons from SGD

Table 3 displays the calculated values of the relative amount of strontium input as well as the relative mass input from groundwater into the lagoons when assuming the waters can be explained by mixing of SGD and Southern Ocean seawater exclusively from equations 1 and 2 respectively. These calculated values from the strontium isotope

($^{87}Sr/^{86}Sr$) and concentration data reflect the salinity decreases observed within the North Lagoon from North to South away and determine high levels of localized mixing of groundwater with seawater.

The calculated Sr input from groundwater (F_{GW}^{Sr}) shows an increase in groundwater discharge from North to South between; Mark Point where salinity and elemental concentration values first begin to decrease from marine values (F_{GW}^{Sr}= 3%) and; Rob's Point where the lowest values of salinity and elemental concentrations within the lagoons was measured (F_{GW}^{Sr} = 37 – 38%). Hypersaline water tested through Parnka Point and in the Northern reaches of the South Lagoon showed the largest fractional input of Sr from groundwater with F_{GW}^{Sr} ranging between 45 – 67% of the strontium content coming from local fresh SGD within these waters. These strontium inputs respectively correspond to relative mass inputs of groundwater *(Using Eq 2)* equal to 12% where groundwater input is first detected in the North Lagoon, a considerable 78 – 80 % near Noonameena, and between 85 – 91 % in the tested South Lagoon samples.

It is most probable and highly feasible that these large calculated values groundwater input into the lagoon are localized phenomena as evidenced by sample NLB11 where no groundwater input was calculated which lies between samples NLB6 and NLB15 where groundwater discharge was detected and water mixing is assumed to be effective over short time periods (~ several days maximum). Furthermore, although not analyzed by their radiogenic Sr isotope signatures ($^{87}Sr/^{86}Sr$), samples SL5(A,B & C) as seen in satellite imagery from GoogleEarth™ in Figure 5 show a good example of this localized effect. Sample SL5A was taken from a water body almost entirely isolated from the

adjacent lagoon water within a large concentric deposition of tufa's, and had a salinity and Sr concentration of only 48.26 PSU and 12.1ppm respectively. In contrast, samples SL5B and SL5C measured approximately 100 and 200m away from SL5C respectively, displayed salinities and Sr concentrations of almost double at 81.55 PSU & 19.0 ppm and 82.50 PSU & 20.4 ppm. This sharp, very local gradient suggests that the groundwater discharge can be localized to very small areas and that active discharge is still occurring within these tufa regions.

5.6 A novel approach to estimating concentration of salinity and strontium via evaporation within the South Lagoon

A novel approach to estimating evaporation effects on salinity and Sr concentrations in the South Lagoon was taken by plotting the South Lagoon samples on the same plot as the hyperbolic mixing trend of the lagoon samples as a mixing of groundwater and seawater primarily. I propose that with the use of the geochemical and isotopic Sr data collected for this study along with the salinity measurements that the concentration factors for hypersaline South Lagoon waters can be estimated based on the following approach. (1) Assuming no radiogenic $^{87}Sr/^{86}Sr$ input from other sources than groundwater during the course of evaporation of the South Lagoon waters, the original Sr composition of the waters can be extrapolated back the hyperbolic mixing curve of mixing between groundwater and seawater, as evaporation will not affect the isotopic ratio of $^{87}Sr/^{86}Sr$. (2) From the projected point on the mixing line the original Sr concentrations are able to be predicted (see figure 10a). (3) By dividing the measured strontium concentration by the predicted value when extrapolated back to the curve, the degree of concentration via evaporation can be predicted (see Table 4 below).

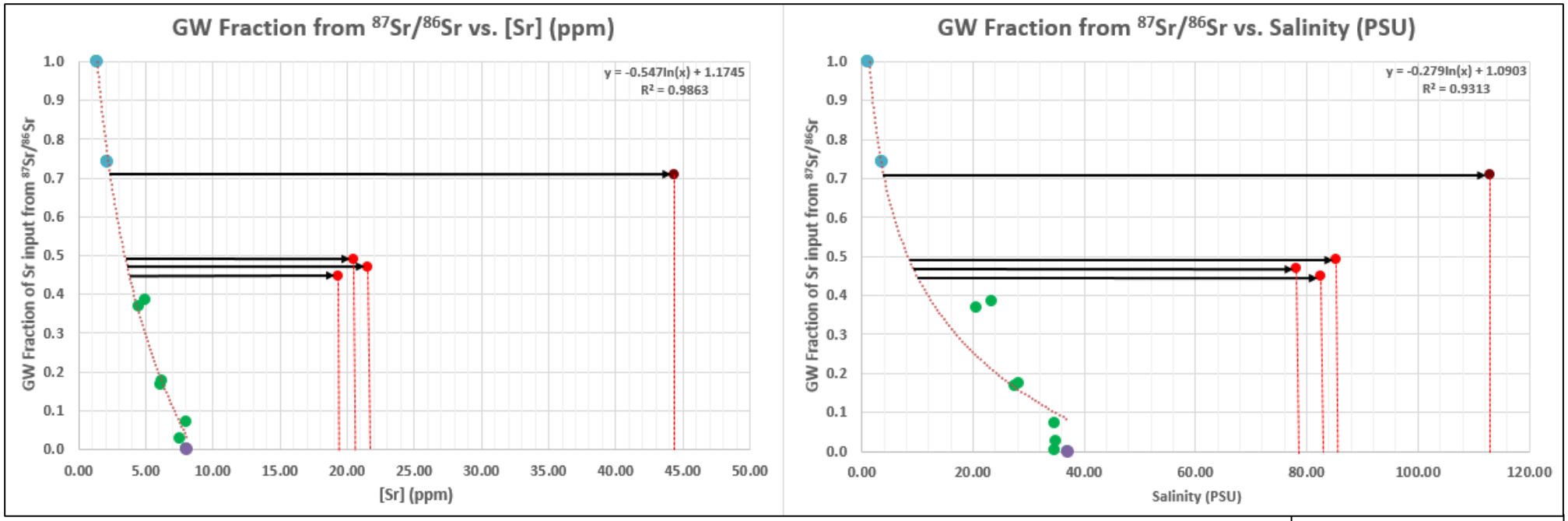

Figure 10: (a) Plot of $^{87}Sr/^{86}Sr$ vs. Strontium concentrations of Coorong lagoon waters displaying hyperbolic mixing trend as shown and discussed in figure 9a. North Lagoon samples including a restricted lake with very low connectivity are included. Black arrows illustrate concentration of Sr via evaporation of samples. Vertical dashed red lines highlight measured Sr concentration values. (b) Plot of $^{87}Sr/^{86}Sr$ vs. salinity of Coorong lagoon waters. Black arrows illustrate a concentration of salinity by evaporation from predicted salinities if they were a product only of their original groundwater – seawater mixture as indicated by their $^{87}Sr/^{86}Sr$ ratios and not of evaporation.

Table 4: Concentration factors in the South Lagoon from original and predicted values of Sr concentrations and salinity's

Sample	F_{GW}^{SR}	Measured [Sr] (ppm)	Predicted Original [Sr] (ppm)	Concentration Factor	Measured Salinity (PSU)	Predicted Original Salinity (PSU)	Concentration Factor
SL1B	0.45	19.31	3.8	5.1	82.55	10.0	8.26
SL2	0.47	21.52	3.6	6.0	78.10	9.3	8.40
SL3	0.64	44.40	2.7	16.4	112.85	5.1	22.13
SL4A	0.49	20.48	3.5	5.9	85.30	8.6	9.92

As can be seen in the table above (Table 4) the concentration factors predicted by Sr concentrations and salinities differ from one another with salinities estimating a higher concentration from evaporation than salinity.

By multiplying the predicted original salinities by the estimated concentration factors we can calculate expected salinities as a test of the reliability of the aforementioned method for predicting concentration from evaporation. Figure 11 (right) shows a plot of these calculated salinities vs. the measured salinity values and shows an underestimation of the true salinity values (indicated by red arrows).

This approach is novel and does not have

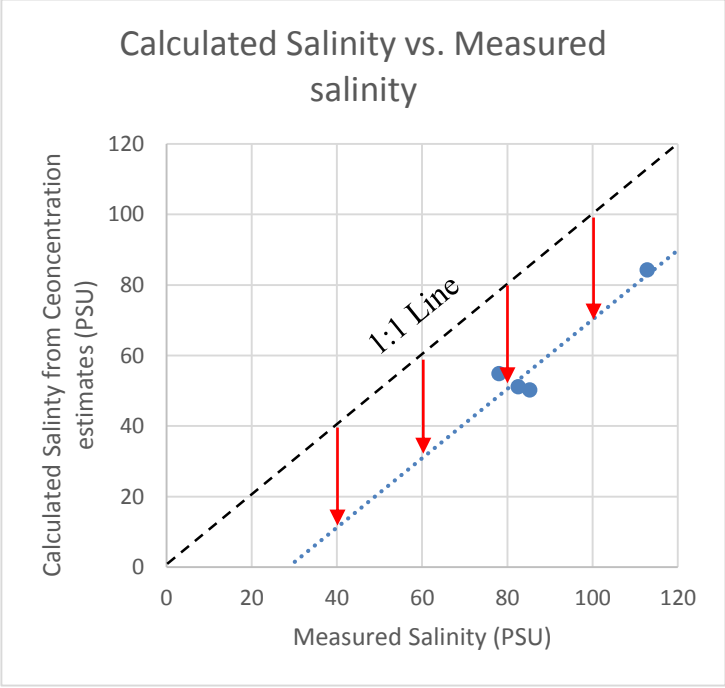

Figure 11: Plot of calculated salinities derived from estimations of concentration factors from evaporation vs. the measured values of salinity within the South Lagoon of the Coorong.

a large enough sample number to properly test the method however I propose it is something which would be worth future investigation as a means of investigating evaporation for the Coorong Lagoons.

6. CONCLUSION

It can be concluded from the results of this study that Submarine Groundwater Discharge (SGD) can have a profound effect on the salinity levels and concentration of major cations of Sr, Ca and Na within the Coorong Lagoons, this effect is masked in the South Lagoon where evaporation rates are high however could be determined with the use of radiogenic strontium isotopes ($^{87}Sr/^{86}Sr$) as a tracer of the groundwater. The results indicated a significant drop of salinity and these elemental concentrations from North to South within the North Lagoon contrary to the well-established trend in literature of salinity purely increasing from North to South. The effects of this SGD into the Coorong appear to be localized.

The SGD detected in this study and measured in Noonameena had significantly different Sr concentration and isotopic $^{87}Sr/^{86}Sr$ signature which allowed for quantitative determination of the contribution of SGD to the overall Sr concentration of the North and South Lagoons and to the water mass of the North Lagoon. The high calculated inputs of SGD to the North Lagoon via isotopic mass balance equations was not measured on both of the lagoon sampling dates at the selected reference point of this study which suggests that the rate of SGD into the lagoons is not consistent and may be related to recharge of the groundwater system, perhaps related to high recharge into the associated aquifer.

Due to the ecological and economic importance of the Coorong Lagoons and the lack of acknowledgment of SGD input into the Lagoons as a significant contributor to the hydrology, it is recommended that further, higher resolution studies are conducted over multiple sampling dates to properly constrain the importance of SGD into the Coorong.

ACKNOWLEDGMENTS

I would like to give acknowledgements to the following people whom, assisted with my project in various ways, this project would not have been completed without their help. Juraj Farkas for his all-round support in the field, and the laboratory, for training me to work with a scientific mentality and for helping me to find a compromise when initial plans were compromised. To Jonathon Tyler for his assistance in the field and ongoing commitment to be present in meetings and share his valuable scientific input. David Bruce for his ongoing support in the clean laboratory and with all things TIMS related. Aoife McFadden at Adelaide Microscopy for her help and the training she provided for solution ICP-MS. To Justin Brookes, for kindly volunteering his time to assist with sample collection and allowing me the use of his boating licence, sampling of the North Lagoon would have been logistically much more difficult without this. Finally to Deborah Haynes, Bronwyn Gillanders, Cameron Barr, Deborah Haynes and John Tibby for their assistance in logistical planning for field sampling.

REFERENCES

BENSON L. & PETERMAN Z. 1996. Carbonate deposition, Pyramid Lake subbasin, Nevada: 3. The use of 87Sr values in carbonate deposits (tufas) to determine the hydrologic state of paleolake systems. *Palaeogeography, Palaeoclimatology, Palaeoecology* **119**, 201-213.

BROOKES J., ALDRIDGE K., DEEGAN B., GEDDES M., GILLANDERS B. & PATON D. 2009. *An ecosystem assessment framework to guide management of the Coorong*. CSIRO.

BUDD P., MONTGOMERY J., BARREIRO B. & THOMAS R. G. 2000. Differential diagenesis of strontium in archaeological human dental tissues. *Applied Geochemistry* **15**, 687-694.

BUTTERMAN W. & REESE JR R. 2003. Mineral Commodity Profiles--Rubidium. **2331-1258**.

CAPO R. C., STEWART B. W. & CHADWICK O. A. 1998. Strontium isotopes as tracers of ecosystem processes: theory and methods. *Geoderma* **82**, 197-225.

CHRIS C., LOCK D. E. & SCHWEBEL D. 1975. Ground-water formation of dolomite in the Coorong region of South Australia. *Geology* **3**, 283-285.

COMMISSION M. D. B. 2006. The Lower lakes, Coorong and Murray mouth icon site environmental management plan 2006-2007. *Living Murray, MDBC Publication*, 115.

FAURE G. 1977. *Principles of isotope geology* (Related Information: Smith and Wyllie intermediate geology series).

FORD T. D. & PEDLEY H. M. 1996. A review of tufa and travertine deposits of the world. *Earth Science Reviews* **41**, 117-175.

GILLANDERS B. & MUNRO A. 2009. Relations between water chemistry, otolith chemistry and salinity of a hypersaline system: implications for determining past environmental history of fish. *CSIRO: Water for a Healthy Country National Research Flagship, CSIRO Canberra, ACT, AustraliaJia YT, Chen YF (2009) Otolith microstructure of Oxygymnocypris stewartii (Cypriniformes, Cyprinidae, Schizothoracinae) in the Lhasa River in Tibet, China. Environ Biol Fish* **28**, 4552Jiang.

GILLANDERS B. M. & MUNRO A. R. 2012. Hypersaline waters pose new challenges for reconstructing environmental histories of fish based on otolith chemistry. *Limnology and Oceanography* **57**, 1136-1148.

HAESE R. R., GOW L., WALLACE L. & BRODIE R. S. 2008. Identifying groundwater discharge in the Coorong (South Australia). 1-6.

HESS J., BENDER M. L. & SCHILLING J.-G. 1986. Evolution of the ratio of strontium-87 to strontium-86 in seawater from Cretaceous to present. *Science* **231**, 979-984.

HOLMDEN C., PAPANASTASSIOU D. A., BLANCHON P. & EVANS S. 2012. δ44/40Ca variability in shallow water carbonates and the impact of submarine groundwater discharge on Ca-cycling in marine environments. *Geochimica et Cosmochimica Acta* **83**, 179-194.

HOPPE K. A., KOCH P. L. & FURUTANI T. T. 2003. Assessing the preservation of biogenic strontium in fossil bones and tooth enamel. *International Journal of Osteoarchaeology* **13**, 20-28.

HORSTWOOD M. S. A., EVANS J. A. & MONTGOMERY J. 2008. Determination of Sr isotopes in calcium phosphates using laser ablation inductively coupled plasma

mass spectrometry and their application to archaeological tooth enamel. *Geochimica et Cosmochimica Acta* **72**, 5659-5674.

KENDALL C. & MCDONNELL J. J. 2012. *Isotope tracers in catchment hydrology*. Elsevier.

KJERFVE B., SCHETTINI C., KNOPPERS B., LESSA G. & FERREIRA H. 1996. Hydrology and salt balance in a large, hypersaline coastal lagoon: Lagoa de Araruama, Brazil. *Estuarine, Coastal and Shelf Science* **42**, 701-725.

KNOPPERS B. 1994. Aquatic primary production in coastal lagoons. *Elsevier Oceanography Series* **60**, 243-286.

KRULL E., HAYNES D., LAMONTAGNE S., GELL P., MCKIRDY D., HANCOCK G., MCGOWAN J. & SMERNIK R. 2009. Changes in the chemistry of sedimentary organic matter within the Coorong over space and time. *Biogeochemistry* **92**, 9-25.

LI H.-C., XU X.-M., KU T.-L., YOU C.-F., BUCHHEIM H. P. & PETERS R. 2008. Isotopic and geochemical evidence of palaeoclimate changes in Salton Basin, California, during the past 20 kyr: 1. δ 18O and δ 13C records in lake tufa deposits. *Palaeogeography, Palaeoclimatology, Palaeoecology* **259**, 182-197.

PALMER M. & EDMOND J. 1992. Controls over the strontium isotope composition of river water. *Geochimica et Cosmochimica Acta* **56**, 2099-2111.

PATON D. C., ROGERS D. J., HILL B. M., BAILEY C. P. & ZIEMBICKI M. 2009. Temporal changes to spatially stratified waterbird communities of the Coorong, South Australia: implications for the management of heterogenous wetlands. *Animal Conservation* **12**, 408-417.

PEARCE C. R., PARKINSON I. J., GAILLARDET J., CHARLIER B. L. A., MOKADEM F. & BURTON K. W. 2015. Reassessing the stable ([delta].sup.88/86Sr) and radiogenic (.sup.87Sr/.sup.86Sr) strontium isotopic composition of marine inputs. *Geochimica et Cosmochimica Acta* **157**, 125.

PEDLEY M., ROGERSON M. & MIDDLETON R. 2009. Freshwater calcite precipitates from in vitro mesocosm flume experiments: a case for biomediation of tufas. *Sedimentology* **56**, 511-527.

PRITCHARD D. W. 1952. Estuarine hydrography. *Advances in geophysics* **1**, 243.

RAIBER M., WEBB J. A. & BENNETTS D. A. 2009. Strontium isotopes as tracers to delineate aquifer interactions and the influence of rainfall in the basalt plains of southeastern Australia. *Journal of Hydrology* **367**, 188-199.

RICHTER F. M. & DEPAOLO D. J. 1988. Diagenesis and Sr isotopic evolution of seawater using data from DSDP 590B and 575. *Earth and planetary science letters* **90**, 382-394.

RICHTER F. M. & LIANG Y. 1993. The rate and consequences of Sr diagenesis in deep-sea carbonates. *Earth and planetary science letters* **117**, 553-565.

RICHTER F. M., ROWLEY D. B. & DEPAOLO D. J. 1992. Sr isotope evolution of seawater: the role of tectonics. *Earth and planetary science letters* **109**, 11-23.

SHAND P., DARBYSHIRE D., LOVE A. & EDMUNDS W. 2009. Sr isotopes in natural waters: applications to source characterisation and water–rock interaction in contrasting landscapes. *Applied Geochemistry* **24**, 574-586.

SHUTTLEWORTH B., WOIDT A., PAPARELLA T., HERBIG S. & WALKER D. 2005. The dynamic behaviour of a river-dominated tidal inlet, River Murray, Australia. *Estuarine, Coastal and Shelf Science* **64**, 645-657.

SINGH S. K., TRIVEDI J. R., PANDE K., RAMESH R. & KRISHNASWAMI S. 1998. Chemical and Strontium, Oxygen, and Carbon Isotopic Compositions of Carbonates from the Lesser Himalaya: Implications to the Strontium Isotope Composition of the Source Waters of the Ganga, Ghaghara, and the Indus Rivers. *Geochimica et Cosmochimica Acta* **62**, 743-755.

SKOUGSTADT M. & HORR C. A. 1960. Occurrence of strontium in natural water. *US Geol. Survey, Circ* **420**, 6.

SMITH J. R., GIEGENGACK R. & SCHWARCZ H. P. 2004. Constraints on Pleistocene pluvial climates through stable-isotope analysis of fossil-spring tufas and associated gastropods, Kharga Oasis, Egypt. *Palaeogeography, Palaeoclimatology, Palaeoecology* **206**, 157-175.

STEIGER R. H. & JÄGER E. 1977. Subcommission on geochronology: convention on the use of decay constants in geo-and cosmochronology. *Earth and planetary science letters* **36**, 359-362.

STEWART B. W., CAPO R. C. & CHADWICK O. A. 1998. Quantitative strontium isotope models for weathering, pedogenesis and biogeochemical cycling. *Geoderma* **82**, 173-195.

TULIPANI S., GRICE K., KRULL E., GREENWOOD P. & REVILL A. T. 2014. Salinity variations in the northern Coorong Lagoon, South Australia: Significant changes in the ecosystem following human alteration to the natural water regime. *Organic Geochemistry* **75**, 74-86.

VIEZER J. 1989. Strontium isotopes in seawater through time: Annual Reviews of Earth and Planetary Science, v. 17.

WANG Z.-L., ZHANG J. & LIU C.-Q. 2007. Strontium isotopic compositions of dissolved and suspended loads from the main channel of the Yangtze River. *Chemosphere* **69**, 1081-1088.

WEBSTER I. T. 2010. The hydrodynamics and salinity regime of a coastal lagoon–The Coorong, Australia–Seasonal to multi-decadal timescales. *Estuarine, Coastal and Shelf Science* **90**, 264-274.

WOLANSKI E. 1986. An evaporation-driven salinity maximum zone in Australian tropical estuaries. *Estuarine, Coastal and Shelf Science* **22**, 415-424.